FEL

Threshold Photoemission Magnetic Circular Dichroism Using Free Electron Laser

T. Nakagawa, T. Yokoyama, M. Hosaka, M. Katoh
Institute for Molecular Science (IMS), Okazaki 444-8585, Japan

Magnetic circular dichroism (MCD) in the x-ray regions (XMCD) has widespread over the synchrotron radiation facilities all over the world because of its high sensitivity to the element specific magnetism. The MCD depends on spin polarization and spin-orbit coupling.[1,2] Since the spin orbit coupling is strong in the core shell and the spin polarization in conduction band is large, x-ray MCD gives large MCD asymmetry. Now its high sensitivity combined with electron microscopy, called XMCD-photoemission electron microscopy (XMCD-PEEM), is used as a very powerful tool for the nano-scale magnetic domain imaging. XMCD-PEEM has been developed into time resolved imaging by using time structure of synchrotron radiation. On the other hand, MCD in the regions from infrared to ultraviolet (UV) is also a useful tool for the study of ferromagnetic ultrathin films. The magneto-optical Kerr effect (MOKE) detects the rotation and distortion of the polarization of reflected lights from magnetic materials. The Kerr effect in valence bands in thin films usually rotates the polarization and changes the ellipticity only by 10^{-2}-10^{-6} rad. This is because of its weak spin orbit coupling, although the spin polarization is large in the valence band. In the valence band photoemission, nevertheless, extensive works have been performed using circularly polarized synchrotron radiation and angle-resolved measurement, showing high (~10%) asymmetry [1,2]. The large asymmetry is attributed to the angle and energy selection of spin orbit split band. This requirement is not suitable for magnetic properties such as magnetization hysteresis curves or magnetic domain imaging because an electron analyzer is inevitable.

We have investigated the observation of enhanced MCD near the Fermi level using visible and ultraviolet lasers in a total yield mode [3]. Figure 1 shows MCD asymmetry as a function of workfunction subtracted by photon energy. Here the workfunction is varied by Cs adsorption and the photon energy is fixed. More than 10% MCD asymmetry is achieved on perpendicularly magnetized 12 ML Ni film on Cu(001), and magnetization curves are obtained. By changing the work function with the aid of cesium adsorption, the laser experiments show that the MCD asymmetry is enhanced only near the photoemission threshold, and that the asymmetry drops to 0.1% for photon energy larger than the work function by 0.6 eV. A theoretical calculation also shows enhanced dichroism near the photoemission threshold, in agreement with the experimental result.

While the above experiment changes workfunction to achieve high MCD asymmetry near the threshold, photon energy tuning is another possibility.

Our experiment needs two properties: *tunable wave length and high photon density*. As shown in Fig.1, to obtain high MCD asymmetry we have to tune the photon energy a little higher than the workfunction. We have used tunable free electron laser from UVSOR-II, which can deliver lower energy than $h\nu$ = 6.3 eV, close to typical workfunction for transition metal surfaces without surface modification such as alkali metal adsorption. Second, MCD method in magnetic field has to be measured by electron drain current from the ground to the sample since the trajectory of emitted electrons strongly depends on the magnetic field. This prevents the use of electron multiplier and needs high light intensity to give sufficient photoelectrons. The FEL in UVSOR can deliver ~100 mW around $h\nu$ = 5 eV [4], which is much stronger than usual laser output in this

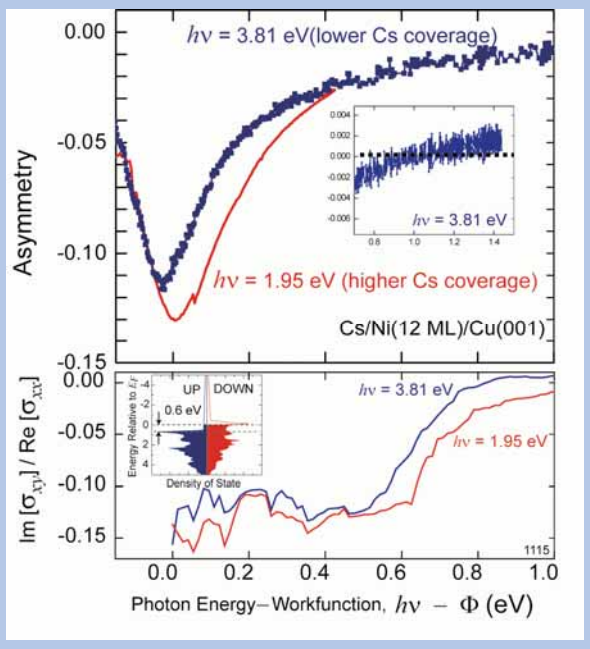

Fig. 1. (top) MCD asymmetry on Ni(12 ML)/Cu(001) surface as a function of workfunction – photon energy. Cs is used to change workfunction. The blue line is for hv = 3.25 eV, while the red 1.95 eV. The inset shows the inversion of MCD sign at 1 eV. (bottom) The corresponding theoretical calculation using Wien2k [6].

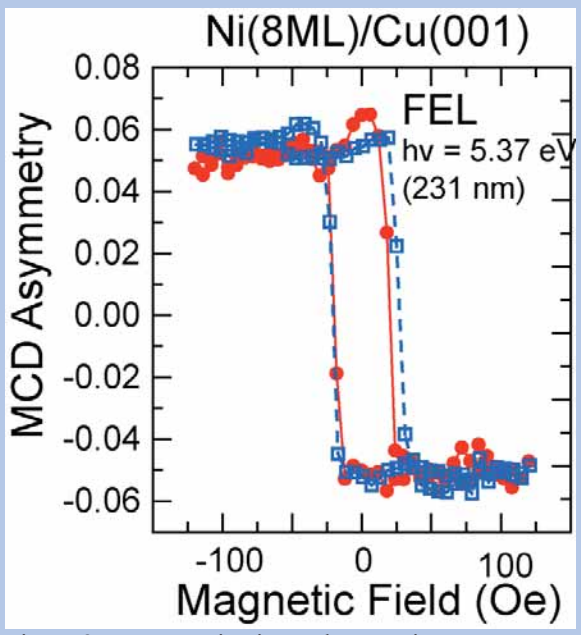

Fig. 2. Magnetization hysteresis curve on Ni(8ML)/Cu(001) taken by FEL-MCD. The plot gives 6% asymmetry. Also shown is the data taken by conventional MOKE.

wavelength region. Furthermore the light is circularly polarized inherently. Owing to its tunability and high intensity, FEL at UVSOR-II is a suitable source to threshold photoemission MCD measurements.

Figure 2 shows a magnetization hysteresis curve on Ni(8 ML)/Cu(001) using $h\nu$ = 5.37 eV, where the photoemission threshold for Ni is ~5.3 eV [5]. As expected from the result shown in Fig. 1, the asymmetry is high, ~6%, near the threshold. This result evidences that the clean Ni surface also shows high asymmetry near the photoemission threshold. The result from conventional magneto-optical Kerr effect is also shown together in Fig.2, having a similar hysteresis shape, which confirms the validity of the MCD method.

MCD in the valence band is strong enough for microscopic measurement. We can measure magnetic domain imaging using photoemission microscopy, which needs high brilliance. Figure 3 shows UVMCD-PEEM result. Unfortunately a FEL-PEEM measurement is still under construction, and here we show a result by a laptop laser. The laser used is LD laser, whose photon energy is 3.06 eV and output power is 5 mW. The magnetic domains (perpendicular to the surface) are clearly visible, giving good contrast. This result promises that FEL is brilliant enough for MCD-PEEM measurements, and MCD-PEEM with FEL is expected to be used for the real time imaging of the magnetic domains under surface modifications.

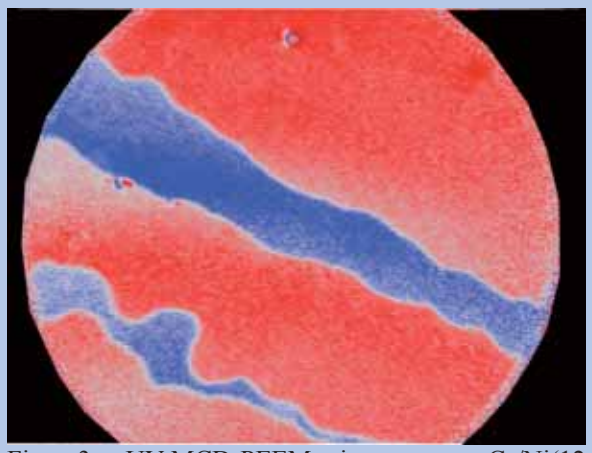

Fig. 3. UV-MCD-PEEM image on Cs/Ni(12 ML)/Cu(001). The field of view is 25 μm. The magnetic domain image is the processed result of the images by the right and left circular light. The red and blue regions are opposite magnetization directions.

[1] C. M. Schneider *et al.*, Phys. Rev. B **44** (1991) R12066.
[2] W. Kuch, C.M. Schneider, Rep. Prog. Phys. **64** (2001) 147.
[3] T. Nakagawa, T. Yokoyama, Phys. Rev. Lett. **96** (2006) 237402.
[4] M. Hosaka *et al.*, Nucl. Instrum. Methods A **483** (2002) 146.
[5] T. Nakagawa *et al.*, Rev. Sci. Instrum. **78** (2007) 023907.
[6] P. Blaha *et al.*, Computer code WIEN2k (Technische Universitat Wien, Vienna, 2002).

BL1A

Performance of CVD Diamond Photon Detectors in the Soft X-Ray Region

Y. Iwakaji, M. Kanasugi, S. Iguchi, O. Maida, T. Ito
Division of Electrical, Electronic and Information Engineering,
Graduate School of Engineering, Osaka University, Suita, Osaka 565-0871, Japan

Introduction

Since diamond with a bandgap of 5.5 eV has such various excellent properties as high breakdown electric field, high thermal conductivity and high chemical stability, it is considered as one of the electronic materials most suitable for high-performance radiation detectors working under severe environments. We have so far been investigating fabrication processes of high-quality single-crystalline diamond films using a high-power MWPCVD (microwave-plasma chemical vapor deposition) method [1], and have reported on performances of photon detectors fabricated with such high-quality diamond films for ultraviolet and soft-X-ray photons with energies below 2 keV [2-4]. In the present study, the room-temperature performance of such CVD diamond detectors has been investigated for soft-X-ray photons of 2.0 – 4.5 keV.

Experimental

Three high-quality homoepitaxial CVD diamond layers (undoped, boron-doped and undoped ones) were grown sequentially on a high-temperature / high-pressure-synthesized Ib (100) diamond substrate with a size of 3×3×0.5 mm^3. The typical thickness of the topmost undoped diamond layers used for the photon detection was ≈50 μm. After the homo-epitaxial growth processes, thin TiN electrodes were formed for the topmost layer using a standard photo-lithography technique and a magnetron sputtering method while Ti/Au bi-layer electrodes were deposited for the buried B-doped layer.

To one of detection areas of the diamond detector thus fabricated, photons with energies of 2.0 – 4.5 keV were irradiated through an aperture of ≈1 mm in diameter. Signal currents were measured at various bias voltages (V_b) of ≤ 100 V. The number of the incident photons was calibrated using a Si photon detector and the temporal storage ring currents.

Results and discussion

Although the number of the incident photons decreased significantly with the increasing photon energy (E_{ph}) in the energy region concerned in this study, the signal currents of the diamond detectors were able to be measured. The quantum efficiency of the photon detector (QE) is given by the quotient of the signal current divided by the product of the element charge and the number of incident photons. Figure 1 shows typical plots of QE versus E_{ph} for two different V_b. On one hand, QE at each E_{ph} is found to increased greatly (abnormally) with increasing V_b. This means that the diamond detector has an important function of increasing amplifications with the increasing V_b, as previously reported [3,4].

On the other hand, at each constant V_b, QE increases with increasing E_{ph} < ≈3 keV, above which QE decreases with increasing E_{ph}. At V_b = 10 V, QE is roughly proportional to E_{ph} below ≈3 keV, which well reflects the number of the electron-hole pairs created in the topmost undoped diamond layer by the incident photons. The critical E_{ph} (≈3 – 3.5 keV) corresponds roughly to the penetration depth of the photons in diamond which equals to the thickness of the detection (topmost undoped diamond) layer. It is also found that QE increases more strongly with the increasing E_{ph} at V_b = 100 V than at V_b = 10 V, indicating that both the location the excited carriers are created and the number of the excited carriers are important factors for the observed signal amplification phenomenon. A possible origin of the amplification is considered to be related to the local high fields formed near the thin TiN electrodes [3,4].

This work was partly supported by the JSPS, Grant-in-Aid for Scientific Research (B) (19360018).

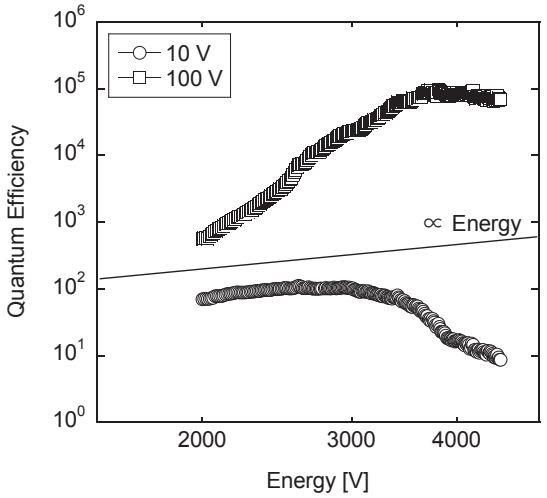

Fig. 1. Photon energy dependence of the quantum efficiency of a diamond detector at the detector bias voltages of 10 and 100 V.

[1] T. Teraji, T. Ito, J. Cryst. Growth **271** (2004) 409.
[2] T. Teraji *et al.*, Diamond Relat. Mater. **13** (2004) 858.
[3] H. Matsubara *et al.*, Diamond Relat. Mater. **16** (2007) 1044.
[4] Y. Iwakaji *et al.*, Appl. Surf. Sci. *in press*.

Evaluation of New Monochromatic Light Sources for ELEPES

G. Funabashi[1], A. Sekiyama[1], H. Fujiwara[1], M. Hasumoto[2], T. Ito[2], S. Kimura[2], P. Baltzer[3], S. Suga[1]

[1]*Graduate School of Engineering Science, Osaka University, Toyonaka, Osaka 560-8531, Japan*

[2]*UVSOR-II, Institute for Molecular Science, Okazaki, Aichi 444-8585, Japan*

[3]*MB Scientific AB, Seminariegatan 29B, SE-75228, Uppsala, Sweden*

In recent years, the extremely-low-energy (< ~12 eV) excitation photoemission study called ELEPES (extremely low energy photoelectron spectroscopy) has attracted much attentions due to its high potential for high bulk-sensitivity and high energy-resolution. However, this technique is not so popular because there are no conventional light sources at present. Therefore, we propose the new monochromatic light sources for ELEPES by means of rare-gas (Ar, Kr, and Xe) resonance lines and the low-energy-pass filters (LiF, CaF_2, and sapphire).

We performed the transmission measurement and the monochromatization experiment at BL1B and BL7B of UVSOR-II, respectively.

Ar I resonance lines appear at ~1040 and 1060 Å. The transmittance limit of LiF is located at ~1040 Å at room temperature (RT). This value is insufficient to realize a single monochromatic line. According to the transmission measurement, the limit wavelength is ~ 1045 Å at ~50 °C which should be sufficient to cut the 1040-Å component. Thus, Ar I resonance lines are monochromatized by LiF heated up to ~50 °C resulting in 1060-Å (11.7-eV) monochromatic light. Kr I resonance lines appear at ~1158 and 1230 Å. The transmittance limit of CaF_2 is located at ~1205 Å at RT and it is sufficient to monochromatize those lines. Thus, we can get the monochromatic light of 1230 Å (10.1 eV) from Kr. Finally, Xe I resonance lines appear at ~1464 Å and below 1300 Å (Fig. 1(a)). The transmittance limit of sapphire is located at ~1430 Å at RT and it is sufficient to monochromatize the lines. We can obtain the monochromatic light of 1464 Å (8.47 eV) from Xe (Fig. 1(b)).

Additionally, we measured the line width of Kr I and Xe I main lines. The line width of Kr I main line was measured not with the highest resolution setting. However, the obtained spectrum can be fitted by a Gaussian curve with the width of 1.34 meV. Considering the resolution, the intrinsic line width is estimated to better than 1 meV. On the other hand, the line width of Xe I main line was measured with the highest resolution setting (E/ΔE~20,000) at the sacrifice of the intensity. The obtained spectrum is fitted by a Gaussian with the width of ~600 μeV (Fig. 1(c)). The energy resolution at this wavelength (1464 Å) is ~423 μeV, so the intrinsic line width of Xe I main line is estimated to be ~426 μeV, which is, at least, much better than 500 μeV.

For the transmission efficiency, the transmittance of 1-mm-thick LiF heated up to ~50 °C is approximately 40% at 1060 Å (Ar I). Those of 1-mm-thick CaF_2 and 2-mm-thick sapphire at RT are approximately 50 and 45% at 1230 (Kr I) and 1464 Å, respectively. The thinner (0.5-mm-thick) filters are expected to be more transparent at each line (Ar I: ~55%, Kr I and Xe I: ~80%). Therefore, we can obtain the monochromatic lines with high intensity by using them.

In conclusion, we proposed the new monochromatic light sources for ELEPES using rare-gas (Ar, Kr, and Xe) resonance and the low-energy-pass filters. Performance test was performed. Thus, it was found that they are useful new ultrahigh-resolution monochromatic light sources for ELEPES.

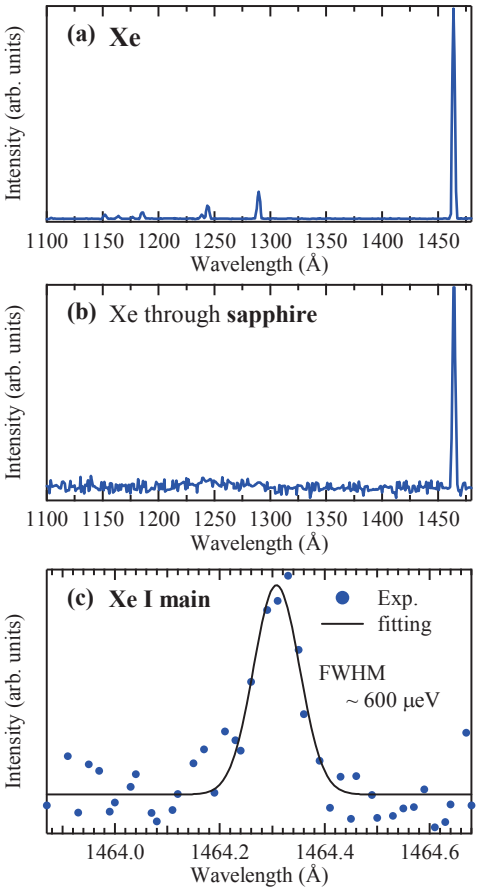

Fig. 1. (a) Xe resonance lines without filter, (b) monochromatized spectrum by using a sapphire filter at RT. (c) Major resonance line of Xe lamp for the highest resolution setting of the monochromator (~20,000).

BL4B

X-Ray Magnetic Circular Dichroism System Using Superconducting Magnet and Liquid He Cryostat

T. Nakagawa[1], Y. Takagi[1], Y. Matsumoto[2], T. Yokoyama[1]
[1]*Institute for Molecular Science, Okazaki 444-8585 Japan*
[2]*Japan Atomic Energy Institute, Tokai, Ibaraki 319-1195, Japan*

Introduction

The X-ray magnetic circular dichroism (XMCD) technique has become matured as a valuable element-specific tool for the determination of microscopic spin- and orbital magnetic moments method. The measurement under high magnetic field and low temperature is substantially important when one wants to investigate, for instance, magnetic anisotropy. This is because saturation magnetization is essential to estimate precisely the spin and orbital magnetic moments along a magnetically hard axis. Since the XMCD system with a superconducting magnet and a liquid He cryostat [1] is not popular around the world especially for public use, we have exploited a new system in this work [2].

Design and Performance

We have designed and fabricated a new XMCD measurement system with a 7 T UHV-compatible superconducting magnet. The system consists of two separated UHV chambers for XMCD measurement and sample preparation. The schematic view and image of the system are depicted in Fig. 1. The sample preparation chamber is equipped with metal evaporators, reflection high-energy electron diffraction (RHEED) or low-energy electron diffraction and Auger electron spectroscopy (LEED/AES) optics, an ion gun, a sample heating system, and so forth. The chamber is evacuated with a turbo molecular pump, a non-evaporation getter pump and a Ti sublimation pump. The base pressure is around 8×10^{-11} Torr.

The measurement chamber was constructed by JANIS Research Company. The system (model 7THM-ST-UHV) consists of a superconducting magnet and a variable temperature insert. The magnet is a 7 T (horizontal field) split multifilamentary NbTi superconducting magnet with a homogeneity of ±0.5% over a 1 cm diameter sphere. The sweep speeds are 1 T/min up to 5 T and 0.25 T/min from 5 to 7 T. A liquid helium reservoir with a 25 l capacity and a minimum of 12 h static hold time (24 h hold time without applying magnetic field) was used.

The sample cryostat has a built in heater and two calibrated Cernox thermometers plus a two-section high-efficiency continuous-flow-type liquid helium transfer line. This offers the lowest sample temperatures of ~4.8 K for accumulated He and ~3.8 K for pumped He.

The sample cryostat can be rotated 360°, allowing us to measure angle-dependent XMCD spectra. A sample holder is a hexagonal Mo with a screw. For future magneto-optical Kerr effect (MOKE) and/or laser-induced photoemission MCD measurements, the chamber possesses several ICF70 viewing ports accessible to the center of the magnet. These ports enable the MOKE measurements with the polar and transverse configurations. The chamber is pumped with a turbo molecular pump, which can be shut down during liquid He insertion. The base pressure is below 2×10^{-10} Torr at the ionization gauge position and should be much lower at the sample position.

The XMCD system was installed at Beamline 4B of UVOSR-II in IMS. The beamline is a bending-magnet soft X-ray station equipped with a varied line spacing grating monochromator, which covers the photon energies of 25–1000 eV. The circularly polarized X-rays were obtained by adjusting the vertical aperture upstream of the first mirror. The circularly polarization factor of P_c=0.70–0.85 can be obtained with a reasonable photon intensity.

The examples of measured spectra can be referred to in this booklet.

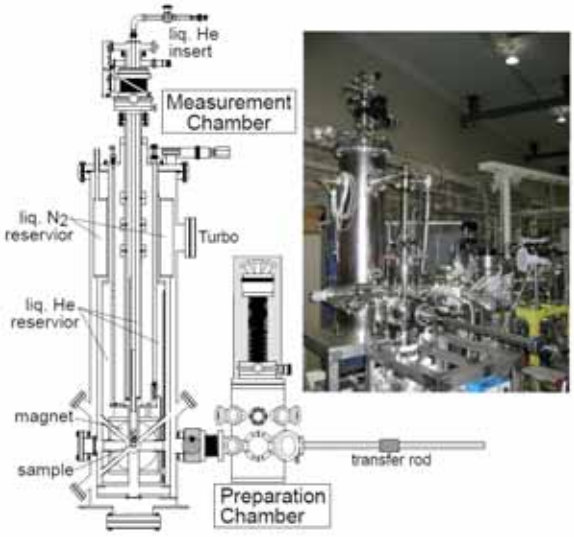

Fig. 1. Schematic rear view and image of XMCD measurement system. The X-rays come from the back surface with a configuration parallel to a magnetic field. The liquid He reservoir with a 25 *l* capacity is surrounded by a liquid nitrogen reservoir with a nominal 10 *l* capacity.

[1] T. Koide, T. Shidara, H. Fukutani, Rev. Sci. Instrum. **63** (1992) 1462.
[2] T. Nakagawa, Y. Takagi, Y. Matsumoto, T. Yokoyama, Jpn. J. Appl. Phys., *in press*.

BL4B

Sensitivity Calibration of a Compact Flat-Field EUV Spectrometer for the Development of Extreme Ultraviolet Light Sources

H. Tanuma[1], H. Ohashi[1], S. Suda[1], S. Fujioka[2], H. Nishimura[2], K. Nishihara[2], T. Kaneyasu[3]

[1]*Department of Physics, Tokyo Metropolitan University, Tokyo 192-0397, Japan*

[2]*Laser Engineering, Osaka University, Osaka 565-0871, Japan*

[3]*UVSOR Facility, Institute for Molecular Science, Okazaki 444-8585 Japan*

Extreme ultraviolet lithography (EUVL) is expected to be used as one of the key technologies in the next generation semiconductor device production. Noting that a Mo/Si multi-layer mirror has the highest reflectivity of about 70% at 13.5 nm of wavelength, a light source peaking of emission around 13.5 nm should be selected for the EUVL technology. For this purpose, a laser-produced plasma (LPP) of tin and xenon is an extremely attractive light source due to its compactness and high efficiency, and it has been investigated both experimentally and theoretically all over the world in this decade [1].

For the understanding of plasmas, spectroscopic data on ions composing the plasmas is definitely required as necessary information. The available spectroscopic data on tin and xenon ions, however, is fairly limited at this moment in time. Publishing works on xenon ions through December 2002 have been compiled by Saloman [2]. Even in this most detailed article about the energy levels and spectral lines of xenon ions, the numbers of levels and lines are not so many and not nearly as good as complete for the multiply charged states. On the other hand, the spectroscopic data of tin ions has not be compiled since the historical work by Moore [3] and is extremely scanty in particular for highly charged states.

In order to provide the fundamental spectroscopic data on tin and xenon ions, we have performed the measurement of various emission spectra from multiply charged tin and xenon ions with charge exchange spectroscopy in Tokyo Metropolitan University [4-6]. In a series of these experiments, we have used a compact flat-field grazing-incident spectrometer, which is equipped with a toroidal-type conversing mirror and a varied line spacing groove grating blazed at 100 nm, and a liquid nitrogen cooled CCD camera as a detector. Efficiencies of the spectrometer and the detector depend on the wavelength. To discuss not only absolute emission intensities also relative intensity distribution, the efficiency should be investigated by experimental measurements.

Absolute efficiency of a similar grating has been studied using bremsstrahlung continuum from LHD (Large Helical Devise) plasmas in NIFS [7], and the sensitivity of a similar CCD has been measured in the synchrotron radiation facility BESSY [8]. However, we wish to know the efficiency of the overall system.

Figure 1 shows a typical spectrum measured in this experiment. This spectrum was observed with injection of 14 nm as the first order light from UVSOR at BL4B with the grating G3 into the compact EUV spectrometer. As can be seen, the prominent peak is at 7 nm. This finding indicates that the second order of the diffraction at the G3 is significant. Not only the higher order light from the G3 but also higher order light from the grating GC in the compact spectrometer can be observed in this figure. For example, the weak peak at 8 nm can be assigned as the 4th order of the GC and the 7th order of the G3.

Because of the very complicated contribution of the higher order lights, the analysis of the obtained data has not be finished at all. We, however, wish to continue the analysis to obtain some results on the higher order diffraction of the gratings and the detection efficiency of the spectrometer.

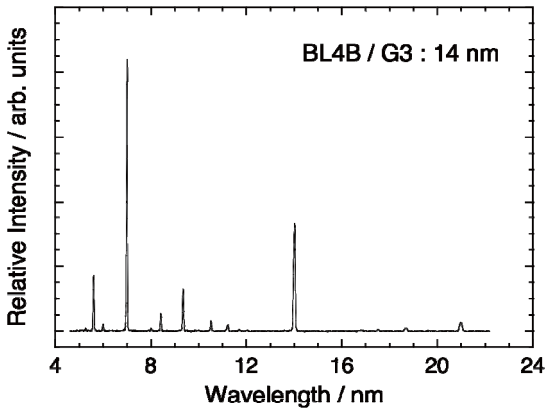

Fig. 1. Observed emission spectrum with injection of 14 nm into a compact EUV spectrometer.

[1] V. Bakshi, "EUV Light Sources for Lithography" (SPIE Press, Washington, 2005).
[2] E. B. Saloman, J. Phys. Chem. Ref. Data **33** (2004) 765.
[3] C. E. Moore, NSRDS-NBS **35** (1971).
[4] H. Tanuma *et al.*, Nucl. Instrum. Meth. B **235** (2005) 331.
[5] H. Tanuma *et al.*, J. Phys. Conf. **58** (2007) 231.
[6] H. Ohashi *et al.*, J. Phys. Conf. **58** (2007) 235.
[7] M. B. Chowdlhuri *et al.*, Rev. Sci. Instrum. **78** (2007) 023501.
[8] G. Schriever *et al.*, Rev. Sci. Instrum. **68** (1997) 3301.

BL5B

Design and Fabrication of Wide-Band Multilayer for 40 – 30 nm Region

T. Goto[1], T. Ejima[1], S. Kimura[2]

[1]*Institute for Multidisciplinary Research for Advanced Materials, Tohoku University, Sendai 980-8577 Japan*

[2]*UVSOR Facility, Institute for Molecular Science, Okazaki 444-8585 Japan*

Monochromators used in the vacuum ultraviolet region (λ<200nm) are normal-incidence one in longer wavelength region (λ>50nm) and grazing-incidence one in shorter wavelength region (λ<50nm) [1], because normal-incident reflectances of conventional mirrors decrease in the shorter wavelength region. Merit of the normal-incidence monochromators is high wavelength-resolution if both types of monochromators can be applied in a same wavelength region. Recently, some reflection multilayers were developed in 50 – 30 nm wavelength region, therefore possibility that normal incidence monochromators will be applied in this wavelength region was suggested [2, 3]. In this study, it were made that design and fabrication of wide-band reflection multilayer mirrors and applying developed-multilayers to the M1 mirror of BL7U at UVSOR-II [4].

Multilayers for normal incidence (ϕ=7.5°) were designed to increase the bandwidth while maintaining the reflectivity in 40 – 30 nm wavelength region. The first step of the design was to select material pairs that show high reflectance in the wavelength region. Among the selected pairs, the pairs to show wide bandwidth of reflectance were chosen. Finally, Mg/SiC pair was remained, because reflection multilayers using this material pair show both high reflectivity and wide band-width. Obtained design parameters are listed in Table 1, and the calculated reflectances using these parameters are shown as solid curves in Figure 1.

The multilayers were deposited on Si substrates (L25.4×W25.4×H10mm) for the M1 mirrors of BL7U beamline using a conventional magnetron sputtering system (ANELVE SPL-500). For evaluation of fabricated multilayer mirrors, the multilayers were deposited simultaneously on Si wafers. Deposition rates were controlled to keep periodic lengths of the multilayers constant in the mirror area. Obtained deposition rate of the Mg deposition was 5.8 nm/min, and of the SiC deposition, 0.87 nm/min in average. The error of the periodic lengths of fabricated multilayers estimated from XRD measurements was ±2% in the mirror area.

Reflectance measurements were made using the G3M4 combination of BL5B beamline. Wavelength resolution λ/Δλ was about 200. Obtained results are shown as squares and triangles in Fig. 1. Squares represent the reflectance of the center of the mirrors, and triangles, of the edge of the mirrors. The peak reflectances of the multilayers are about 0.3, and its values between the center and the edge of the mirrors are nearly equal to each other. Fabricated 4 multilayer mirrors cover 43 – 28 nm wavelength region with that their reflectances are 0.2 or more. These multilayer mirrors were installed in the M1 mirror of BL7U beamline. Throughput of this beamline in this wavelength region was about 10 times or more greater than the previous one, which used conventional Au mirror as the M1 mirror [4].

Table 1. Design parameters for wide-band multilayers in 40 – 30 nm wavelength region.

Multilayer No.	Periodic number	Periodic length D (nm)	Thickness ratio $\gamma=d_{SiC}/D$
1	7	16.6	0.42
2	7	18.0	0.41
3	6	19.8	0.40
4	6	22.2	0.40

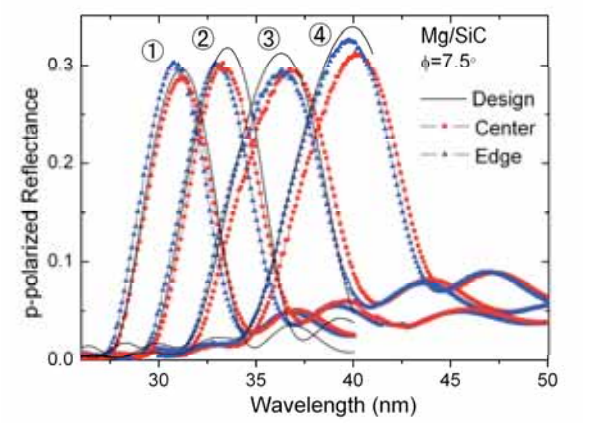

Fig. 1. Calculated and measured reflectances of wide-band multilayer mirrors. Numbers at the peaks represent the multilayer number in Table 1.

[1] Vacuum Ultraviolet Spectroscopy II, edited by J. A. Samson, D. L. Ederer (Academic Press, San Diego, CA, 2000), Chap. 1 & 2.

[2] Y. A. Uspenskii *et al.*, Optics Letters **23** (1998) 771.

[3] T. Ejima *et al.*, Jpn. J. Appl. Phys. **40** (2001) 376.

[4] S. Kimura *et al.*, UVSOR activity report 2006 (2007) 50.

BL5B

Evaluation of Higher Order Diffraction Light Contaminations at EUV Region by Using Transmission-Grating Spectrometer

F. Suzuki[1], T. Ito[1], K. Fukui[1], T. Hatsui[2], N. Kosugi[2]
[1]*Dept. Elec. Elec. Engi., Univ. of Fukui, Fukui 910-8507, Japan*
[2]*Institute for Molecular Science, Okazaki 444-8585, Japan*

Absolute measurement of physical properties generally requires quantitative information on the unwanted higher diffraction-order intensity in light sources. However, there are many difficulties to evaluate the higher diffraction-order intensity in EUV region. The energy analysis of the photoelectron emitted from the appropriate material which is irradiated by the target monochromatized light is one way to realize the evaluation of the higher-order contaminations, but the composition of the photo-electron spectrometer is complicated and the operation is not so easy. Another way to realize the evaluation is using the second monochromator. It means that the target monochromatized lights by the first monochromator are monochromatized again by the second monochromator. In EUV region, however, this method also has the difficulties, because the diffraction efficiency of the reflectance grating under the grazing incidence condition is quite sensitive to the incidence angle. On the other hand, the diffraction efficiency under the normal incidence is not sensitive. However, the normal incidence condition in EUV region is only achieved by the use of transmission grating which is very difficult to fabricate. In this experiment, our object is to present a simple but precise method for the evaluation by using the compact transmission grating spectrometer (CTGS).

A CTGS is equipped with a quasi-free-standing transmission grating with groove density of 5882 l/mm made by electron-beam lithography and a nickel electroplating method. The collimated mono-chromatized light by both the 100 um aperture and a 100 um entrance slit is re-monochromatized by the transmission grating which is located just behind the entrance slit. The re-monochromatized light is detected by the silicon photodiode (SPD) which is mounted on the linear motion stage. This stage is apart 196.5 mm from the grating and is able to move along to the dispersion direction of the grating.

The present method has been first applied to the plane-grating monochromator beamline (BL5B). Figure 1 shows the typical spectrum observed by the CTGS. The incident light is monochromatized 17.8 nm by the G2-M22 configuration of BL5B. The peak at 17.8 nm is basically denoted as (1 - 1) peak, where the label is denoted as (diffraction order of the monochromatized light by PGM – diffraction order of the re-monochromatized light by CTGS). The peaks at 8.9 nm and 5.9 nm are labeled as (2 – 1) and (3 – 1) peaks, respectively. Fig. 1 also suggests that (4 – 1) peak is negligible small. In other word, 17.8 nm light under G2-M22 configuration has up to 3rd order contaminations. Then, 17.8 nm peak is definitely labeled as (1 – 1)+(2 – 2)+(3 – 3) peak, and 26.7 nm peak as (2 – 3) peak. By measuring spectral profile of EUV light from G2-M22 configuration at each wavelength using CTGS, higher diffraction- order light intensity in EUV light source, and dependence of CTGS efficiencies on wavelength, are determined self-consistently. The results assume only the detection efficiency of SPD (IRD Inc., AXUV-100). Figure 2 shows number of the photon ratio r_n of the n-th diffracted contamination to the 1st order light at the G2-M22 configuration of BL5B. Fig. 2 represents the purity of the monochromatized light under G2-M22 configuration is good at shorter wavelength side and is consistent with the optical design of BL5B.

.

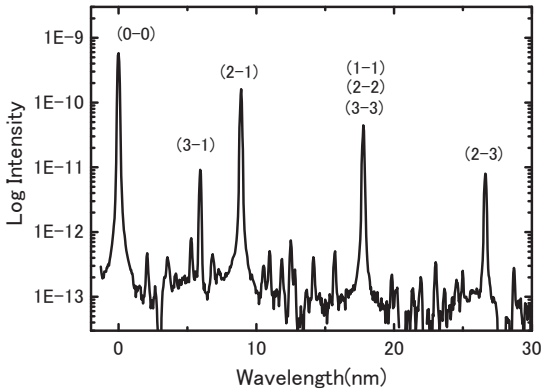

Fig. 1. Typical spectrum of the CTGS at 17.8 nm.

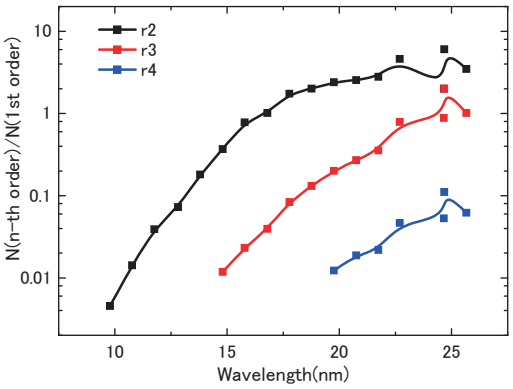

Fig. 2. Number of the photon ratio r_n of the n-th diffracted contamination to the 1st order light at the G2-M22 configuration of BL5B.

BL5B

Measurement of Absolute Efficiency for Micro Channel Plates by Using Pure-Calibrated EUV Beam

K. Yoshioka[1], G. Murakami[1], T. Toyota[1], G. Ogawa[1], A. Yamazaki[2], I. Yoshikawa[1]
[1]*Department of Earth and Planetary Science, Graduate School of Science, The University of Tokyo, Tokyo 113-0033 Japan*
[2]*Institute of Space and Astronautical Science, Japan Aerospace Exploration Agency, Sagamihara, Kanagawa 229-8510 Japan*

Introduction

We study the tenuous atmosphere of the planet Mercury thorough the optical observations. One of the main components of the atmosphere is helium. The atom has resonance scattering emission lines in the extreme ultraviolet (EUV) region, at 58.4nm. The intensity of the emission is proportional to column density of the scattered particle under the assumption of the optically thin condition. The information of the amount and the distribution of helium are crucial for discussing about the current environment and the evolution of the planet.

The Mercury Planetary Orbiter (MPO) in the BepiColombo mission will be launched in 2013 and put into the orbit around the Mercury after 6.5-year-long cruise. An ultraviolet Spectrometer, PHEBUS (Probing of Hermean Exosphere by Ultraviolet Spectroscopy) that is loaded onto the MPO will observe the atmosphere of Mercury in the EUV and FUV (far ultraviolet) region from the Mercury orbit. In our experiment, in order to calibrate the sensitivity of the PHEBUS, we measure the quantum efficiency of the micro channel plates (MCPs) which we use as the standard detector, at 58.4nm line.

Measurement and Result

We install a Sn (354.5nm) filter on the entrance of the SOR beam to eliminate the multi-order lines from the 58.4nm line with PGM35. At first, we investigate the purity of the 58.4nm line through the Sn filter. We judge the purity from the consistency between the wavelength characteristics of an Sn (173nm) filter for the particular lines at the EUV facilities of Institute of Space and Astronautical Science (ISAS) and those for the continuous lines at UVSOR. The former is measured for the emission lines of the helium gas with the discharge light source. Fig. 1 shows the transmittances of the filter measured at ISAS and UVSOR. It is clear that transmittances of the filter are consistent around the wavelength 58.4nm. We interpret from the result that the pure 58.4nm can be introduced through the Sn filter by using PGM35.

With the available pure 58.4nm line, then we measure the quantum efficiency of the MCPs. The quantum efficiency is calculated by the rate of the MCPs count to the electron yield of the photo diode which is absolutely calibrated. The result of the measurement shows that the quantum efficiency of the MCPs is 11.9±1.4% at 58.4nm line.

As the next step, in addition to the 58.4nm line, we plan to measure the quantum efficiency at the 73.4nm and 83.4nm lines, which are other observational objects of PHEBUS (73.4nm is the emission line of Neon and 83.4nm is that of the ionic oxygen). Then the purities of 73.4nm and 83.4nm lines are essential, and must be investigated for the next machine time.

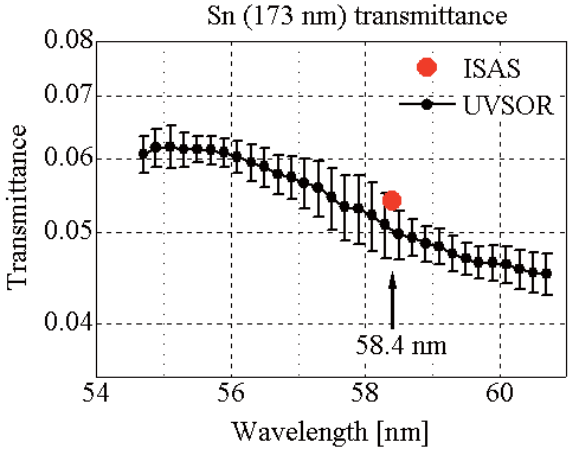

Fig. 1. The transmittances of a Sn (173nm) filter. The red dot shows the results of the measurements at the EUV facility of ISAS (the error is smaller than the dot size) and the solid line with dots shows that at UVSOR.

BL6U

Design of a New Monochromator for BL6U

E. Shigemasa[1], Y. Hikosaka[1], E. Nakamura[1], N. Kondo[1], T. Horigome[1], K. Amemiya[2]
[1]*UVSOR Facility, Institute for Molecular Science, Okazaki 444-8585 Japan*
[2]*Photon Factory, Institute of Materials Structure Science, Tsukuba 305-0801 Japan*

Various types of monochromators for synchrotron radiation have been proposed and constructed to realize vibrational spectroscopy in the soft x-ray range (100 ~ 1000 eV), which contains the *K*-shell thresholds of chemically important elements like C, N, and O, since the first successful observation for the vibrational structures of the π* resonance in the *K*-shell photoabsorption spectrum of nitrogen molecules [1]. Thanks to the high brilliance offered by undulator radiation, both high-resolution and high-flux are achievable simultaneously at a considerable high level. At the UVSOR, there is only one soft X-ray undulator beamline for high resolution spectroscopy, BL3U, in the photon energy region of interest.

Concerning the utilization of the first in-vacuum type undulator, which has been relocated from the long straight section U7 to the short one between B05 and B06, a new project for constructing the undulator beamline BL6U has been initiated. We have decided to choose the entrance slit-less configuration for the monochromator. A varied-line-spacing (VLS) plane grating monochromator (PGM) seems to be one of the most trustworthy ones to realizing high resolution in the soft x-ray range. In order to cover a wide photon energy region (30-500 eV) with one single grating, a variable-included-angle Monk-Gillieson mounting VLS-PGM [2], in which the grating is illuminated by converging soft X-rays, has been selected. Design study for the monochromator at BL6U has been completed, with the collaboration of KEK-PF. The monochromator designed will cover the photon energy ranging from 30 to 500 eV, with the resolving power higher than 10000 and the photon flux more than 10^{10} photons/sec.

Figure 1 shows a schematic layout of the optical elements of the present VLS-PGM. In front of all optical elements, there is an aperture S_0, located 5.0 m from the source position. The usual setting of this aperture is 2.0 mm^V × 2.0 mm^H, which limits the half acceptance angle to 0.4 $mrad^V$ × 0.4 $mrad^H$. The radiation is deflected horizontally by a toroidal mirror M_0 located 1.5 m downstream of the aperture. M_0 is one of the most important optical elements to realizing high resolution, which essentially focuses the radiation onto an exit slit S_1, and converging soft X-rays illuminate the VLS grating indicated by G. A plane mirror M_1 is located 1.5 m behind M_0. M_0, M_1, and G (Si substrates) are cooled from both sides by water-cooled copper alloy blocks. One laminar profile plane grating, which is ruled holographically, with the varied-line-spacing, is designed to cover the energy range from 30 eV to 700 eV. The groove density of the grating is 500 l/mm at its center position. The included angle of the grating should be changed from 167° to 176° in order to minimize the aberrations. A refocusing mirror M_2 has a toroidal shape, which focuses the monochromatized radiation at the sample position. All the grating and mirrors are coated with Au.

The resolution of the present monochromator was studied by ray-tracing simulation as well as analytical estimation. As a result, it is found that a resolving power E/ΔE of more than 10000 is achievable over the energy range from 30 to 500 eV with one single grating having the groove density of 500 l/mm. The throughput photon flux estimated ranges from 10^{10} to 10^{12} photons/sec for the ring current of 350 mA, with a resolving power of 10000. The practical construction of BL6U is expected to start from the summer of 2008.

[1] C. T. Chen, Y. Ma, F. Sette, Phys. Rev. A **40** (1989) 6737.
[2] K. Amemiya. T. Ohta, J. Synchrotron Rad., **11** (2004) 171.

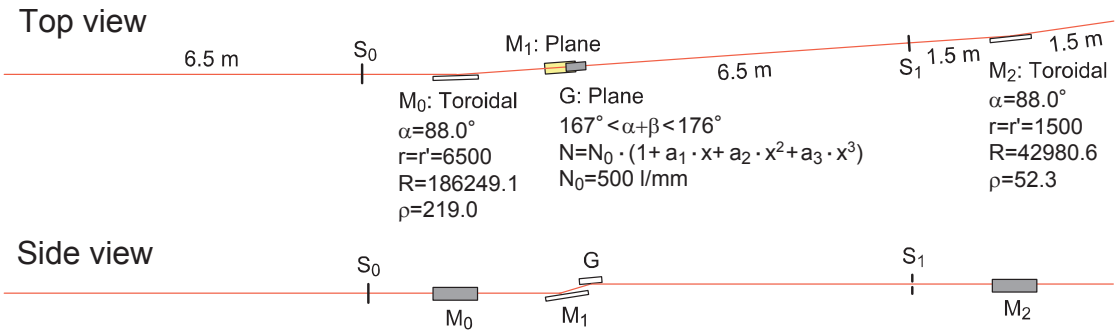

Fig. 1. Schematic layout of the monochromator designed for BL6U.

BL7U

Performance Test of High-Throughput Three-Dimensional Angle-Resolved Photoemission Spectroscopy at BL7U

T. Ito[1,2], S. Kimura[1,2], M. Sakai[1]

[1]*UVSOR Facility, Institute for Molecular Science, Okazaki 444-8585, Japan*

[2]*School of Physical Sciences, the Graduate University for Advanced Studies (SOKENDAI), Okazaki 444-8585, Japan*

In FY2006, we have constructed a new VUV beamline BL7U equipped with a three-dimensional angle-resolved photoemission (3D-ARPES) apparatus [1]. The aim of this beamline is to investigate the anisotropic interaction at the Fermi surface (FS) of inter-metallic compounds [1], namely "Fermiology", which is one of the most facilitated research fields in recent days, since the interactions among carriers, local spins, and lattice vibrations play a dominant role in the functionality of materials. After adjustment of the beamline and ARPES apparatus, we realize high-throughput 3D-ARPES beamline for the bulk-sensitive Fermiology of strongly correlated electron systems (SCES).

The BL7U equips an APPLE-II-type undulator for the VUV light source, a Wadsworth-type VUV monochromator, a multi-channel electron energy analyzer (MBScientific AB; 'Peter' A-1) and a liquid-helium flow-type cryostat with a 6-axis manipulation system (R-dec Co. Ltd.; i-Gonio). The light source and monochromator provide high-energy resolution ($E/\Delta E \geq 10^4$) with high photon flux ($\geq 10^{12}$ ph/s). The definition of the 6-axis of the manipulator are illustrated in Fig. 1.

Figure 2 shows a 3D-ARPES result on a strongly correlated 4f electron compound CeSb. With tuning sample tilting (θy) as well as photon energy (hν), we have successfully mapped out the 3D FS topology of cigar-shaped hole-like FS at the X point (image plot in Fig. 2), which is well reproduced by the band calculation (3D illustration in Fig. 2). It should be noted that the acquisition time of the present three dimensional (3D) FS image together with the 3D band structure is within 6 hours. The present high-throughput measurement can be realized by the wealth of the high-photon flux at BL7U as well as the 6-axis sample manipulation systems.

The present result clearly indicates that the VUV 3D-ARPES gives us a detective information of bulk 3D electronic structure which can be compared with band calculations. Furthermore, this method makes it possible to elucidate the origin of various functionalities through the direct observation of anisotropic interactions as quasi-particle band dispersions. In turn, it also derives a key for opening a new research field of *functionality design* by understanding the essential origin of various functionalities in the future.

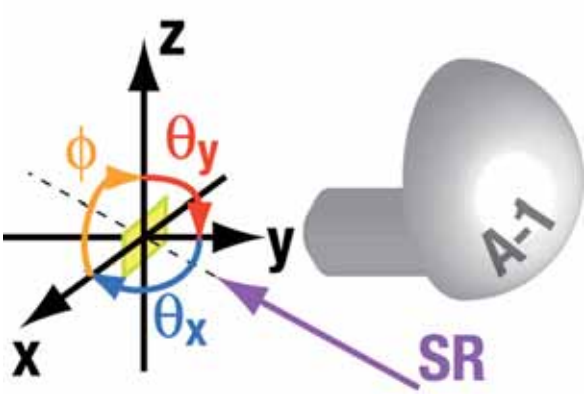

Fig. 1. The definition of 6-axis of the manipulator with respect to a sample (yellow square) together with the experimental layout of 3D-ARPES.

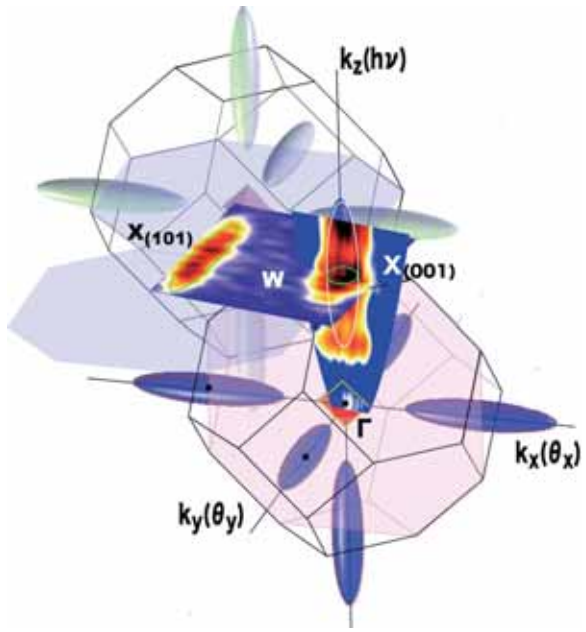

Fig. 2. 3D-FS image of CeSb obtained by mapped out the 3D-ARPES intensity at the Fermi level. 3D illustration of calculated FS is also depicted.

[1] S. Kimura *et al.*, AIP Conf. Proc. **879** (2007) 527.

BL8B1

Characterization of Mo/Si Multilayer Mirror for Time-Resolved Spectroscopy with Laser High Order Harmonic Pulses

M. Fushitani[1,2], A. Matsuda[1], A. Hishikawa[1,2,3]

[1]*Dept. of Photo-Molecular Science, Institute for Molecular Science, Okazaki 444-8585, Japan*

[2]*Dept. of Physical Sciences, The Graduate University for Advanced Studies (SOKENDAI), Okazaki 444-8585, Japan*

[3]*PRESTO, Japan Science and Technology Agency, Saitama 332-0012, Japan*

Recent advances in laser technology have allowed us to generate laser high-order harmonics (HH) in the soft X-ray region by focusing intense femtosecond infrared (IR) laser pulses to gaseous nonlinear media [1]. The laser HH pulses have characteristic features as 1) high photon energies extending up to the keV region, 2) ultrashort pulse duration on an attosecond timescale, 3) high photon flux comparable to synchrotron radiation, and 4) simple and precise synchronization of other laser light sources. Because of these aspects, the laser HH pulses are of great interest as a potential light source for time-resolved spectroscopy of ultrafast dynamics of electrons and nuclei that could not be elucidated in real time by conventional techniques.

To fully utilize the characteristics of laser high-order harmonics, appropriate optical components need to be employed. The laser HH pulses consist of odd order harmonics with different photon energies below the "cut-off" [1]. The harmonic-order (or wavelength) selection could be achieved by using a grating with large incident angles. In this case, however, the time resolution will be significantly reduced because of the pulse stretching due to large optical path differences. To keep pulse duration as short as possible, multi-layer coated mirrors are preferable. Among them, the molybdem/silicon (Mo/Si) multilayer has been widely used as a reflective coating for optical mirrors in the 13 nm (95 eV) region. In order to use one of the harmonics, Mo/Si multilayer mirrors with a narrow band width can be fabricated in such a way that only the selected harmonic pulse is reflected. In the present study, we characterize reflectance of Mo/Si multilayer mirrors at small incident angles.

The reflectance measurements of Mo/Si multilayer mirrors (NTT-AT Inc.) were performed at BL8B1. The synchrotron radiation, which was dispersed by the G3 grating (360 l/mm), was measured as reference light simultaneously by using gold (Au) mesh and Si photodiode (AXUV100, IRD Inc.) detectors in an energy range of 30~140 eV. The energy scale was calibrated with a sharp absorption edge of an aluminium (Al) filter (a thickness of 120 nm, Luxel Inc.) at 72.7 eV as well as that at 36.3 eV due to the second order light from the grating. From the transmission of the Al filter around the 90 eV region, the higher order light contribution was estimated to be less than 4 % of the total current of the Au and Si detectors. The light reflected by the Mo/Si multilayer mirror was detected at various incident angles of 5~27.5 degree by using the Si photodiode. The light before reflection was also monitored by the Au mesh, by which the intensity of incident light with respect to that of the original reference light is normalized at each wavelength.

Figure 1 shows reflectance of a Mo/Si multilayer mirror as a function of photon energy. The incident angle (θ) was varied from 5 to 27.5 degree with a step of 2.5 degree. The reflectance was determined to be 60 %, irrespective of the incident angle except for θ = 27.5°. The reflectance peak shifts toward the higher energy side while the band width becomes narrower as the incident angle increases. For θ = 5°, the peak position and the full width at half maximum of the reflectance were determined to be 89.6 eV and 2.8 eV, respectively. In this arrangement, the Mo/Si mirror selectively reflects the 59th harmonic (89.7eV) of an IR laser pulse at 815 nm (1.52 eV).

We are very grateful to the staff of the UVSOR facility.

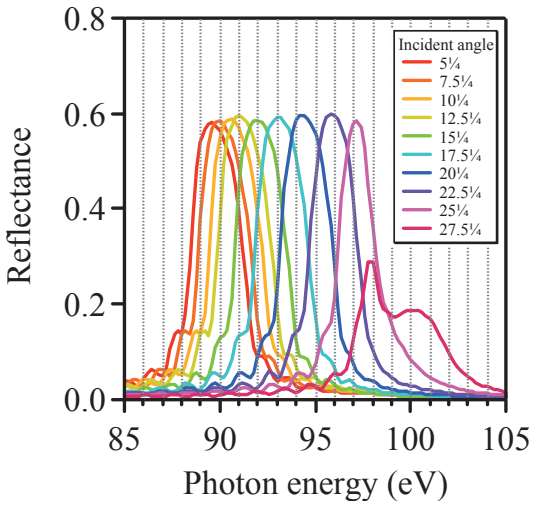

Fig. 1. Reflectance of Mo/Si multilayer mirror at incident angles between 5 and 27.5 degree.

[1] T. Brabec, F. Krausz, Rev. Mod. Phys. **72** (2000) 545.